Characterization of Sol-gel Prepared Silica Supported NiO-CuO Composites

[1]Samreen Zahra*, [2]Dr. Narjis Naz, [3]Dr. Muhammad Zia-ur-Rehman, [4]Muhammad Irfan
[1]Asma Sheikh and [2]Sania Izhar
[1]*Mineral Processing Research Centre, PCSIR Laboratories Complex, Ferozepur Road,
Lahore-54600, Pakistan.*
[2]*Department of Chemistry, Lahore College for Women University, Jail Road, Lahore-54610, Pakistan.*
[3]*Applied Chemistry Research Centre, PCSIR Laboratories Complex, Ferozepur Road,
Lahore-54600, Pakistan.*
[4]*Pakistan Institute of Technology for Minerals and Advanced Engineering Materials,
PCSIR Laboratories Complex, Ferozepur Road, Lahore-54600, Pakistan.*
samreenzahra68@hotmail.com*

Summary: Silica (SiO_2) supported nickel oxide-copper oxide (NiO-CuO) composites were synthesized through alkoxide route of sol-gel process using tetraethyl orthosilicate (TEOS), nickel nitrate hexahydrate and copper nitrate trihydrate as precursors. A series of different compositions were prepared varying NiO:CuO molar ratios keeping all other process parameters constant. The gels thus obtained were calcined at a moderate temperature i.e. 500ºC for one hour. The crystal structure and thermal stability of metal oxide particles embedded in silica matrix were studied using X-ray diffraction technique (XRD) and differential scanning calorimetry (DSC-TGA) respectively. The purity of the composites was checked by Infrared spectroscopy (IR) whereas the composite formation was confirmed by scanning electron microscopy. The results revealed that crystals of NiO and CuO nanoparticles aggregated to form spheres of variable sizes were successfully embedded in the amorphous silica matrix composed of silica particles agglomerated to form clusters.

Keywords: Nickel-copper oxide; Composites; Alkoxide route; Sol-gel; Silica matrix.

Introduction

Composites comprising of ultrafine metal and metal oxide particles supported on vitreous matrices possess a variety of outstanding properties that are immensely size-dependent [1-3]. Because of their high surface area, good chemical stability, enhanced thermal, electrical, mechanical, optical and magnetic properties, these composites found extensive application in humidity and gas sensors, organic catalysis, solar cells, magnetic and electronic devices and automobile industry [4, 5]. Among various methods employed for synthesis of these materials, sol-gel is the most promising technique which allows modification of material properties simply by varying process parameters [6]. In the last few years, many researchers have successfully synthesized metal oxide nanoparticles, metal oxide nanocomposite powders and also, highly developed coating films with controlled porosity and homogeneous distribution of particles in the nanostructures through sol-gel process [4, 7-14].

Catalysts and adsorbents of large pore structure and high surface area can also be produced through sol-gel route. Bimetallic catalysts usually having transition metal oxides supported on silica or alumina appreciably enhance the catalytic properties of the hybrid material owing to the structural and electronic effects induced by one metal into the other.

It has been observed that no substantial change in the pore diameter of silica nanoparticles occurs at low calcination temperatures and they have high specific surface area upto 600-700ºC, thus smaller crystallites may be formed by co-precipitation of metal oxide precursors on the surface of silica matrix [15]. Scientists have therefore developed various compositions of nanocomposites that are composed of mixed metal oxides and found them active catalysts for processes like steam reforming of ethanol and oxidation of alcohols to aldehydes and ketones [16, 17]. Jeong *et al*. studied the catalytic activities of Ni-based catalysts supported on TiO_2-SiO_2 xerogel and derived the most suitable composition for 100% conversion efficiency for oxidation of acetalaldehyde [18]. Recently, researchers have found NiO-CuO nanocomposites to be cytotoxic and antifungal as well [19].

One of the novel properties of nanostructured metal oxides is their optical activity [20] which is believed to be important with respect to their use in gas sensors. The optical transmittance of nanoparticles, nanocomposites composed of mixed metal oxides embedded in silica matrix, or thin films changes on exposure to gases like H_2S, NO_x, CO and H_2. Silica films doped with nanocrystals of metal oxides provide large surface area which leads to

---

*To whom all correspondence should be addressed.

enhanced gas sensing properties [21-23]. Gold particles in combination with NiO, CuO and Co_3O_4 also affect optical gas sensing [24, 25]. Moreover, heat treatment conditions during preparation, residual porosity and temperature during exposure to gases affect the performance of these nanocomposites [26]. Nickel oxide nanoparticles alone because of their large band gap energy have been found to be less active towards optical response; therefore, nickel oxide particles embedded in an insulating matrix like silica have been suggested for enhanced optical properties [27]. Furthermore, silica can be a perfect support for magnetic nanoparticles like NiO, the reason being it can avoid the magnetic anisotropic dipolar attraction when external magnetic field is not present [6].

In the present study, different compositions of NiO-CuO particles embedded in silica matrix were fabricated by sol-gel process which is the most feasible method being simple, cheap and environment friendly. The prepared composites were characterized by X-ray diffraction technique, differential thermal analysis, infrared spectroscopy and scanning electron microscopy. Aim of the study was to investigate the variation in physical characteristics of silica supported NiO-CuO particles by varying their composition.

Experimental

Materials

Tetraethoxysilane (TEOS) (Fluka), nickel nitrate hexahydrate (Merck) and copper nitrate trihydrate (Merck) were used as silica, nickel oxide and copper oxide precursors respectively. The catalyst used was nitric acid (Merck) whereas absolute ethyl alcohol was used as solvent.

Sample Preparation

Different compositions of NiO-CuO/SiO_2 composites were synthesized by alkoxide route of sol-gel process shown in the flowchart (Fig. 1).

The sols were prepared by dissolving measured quantities of nickel nitrate hexahydrate and copper nitrate trihydrate in a mixture of ethanol and water taken in 2:1 ratio. The pH was maintained at 1 using nitric acid. TEOS was then added dropwise to the mixture at 60ºC temperature with constant stirring for one hour. The prepared gels were dried at 60ºC for 18 hours and after grinding the samples were calcined at 500ºC for one hour. Three compositions (NCS-1, NCS-2, and NCS-3) with variable quantities

of NiO and CuO and fixed quantity of SiO_2 were prepared which are presented in Table-1.
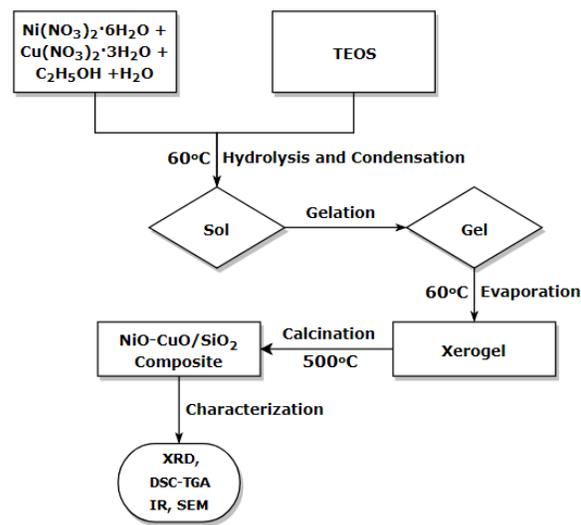

Fig. 1: Schematic representation of sol-gel processing.

Table-1: Compositions of SiO_2 supported NiO-CuO composites.

Sample ID	Molar ratios NiO:CuO:SiO_2	Quantities of precursors added		
		Ni(NO₃)₂·6H₂O (g)	Cu(NO₃)₂·3H₂O (g)	TEOS (g)
NCS-1	3:1:6	5.89	1.53	10.72
NCS-2	1:1:3	3.93	3.05	10.72
NCS-3	1:3:6	1.96	4.58	10.72

Characterization

Nanocrystals of NiO and CuO embedded in silica matrix were characterized by Bruker X-ray diffractometer (D8 Advance) using monochromatised $CuK_{\alpha}1$ radiation having wavelength of 1.54060Å. Thermal analysis was carried out using differential scanning calorimeter Universal V4.5A, TA instruments USA, under nitrogen atmosphere from room temperature to 1000ºC at a rate of 10ºC/min. Infrared spectroscopy was performed with Thermo Nicolet IR 200 (USA), the samples were scanned through Zinc Selenide (Zn-Se) ATR. Surface morphology was studied using scanning electron microscope S-3700N Hitachi Japan.

Results and Discussion

NiO-CuO/SiO_2 composites were prepared via sol gel process varying NiO-CuO molar ratios and keeping ethanol-water ratio, pH, stirring time and calcination conditions constant. For preparing a composite, the matrix selected should not be reactive

towards the metal oxide [15]. Since, silica is a neutral oxide so it has been selected as a support in the present study. It has been observed that water content, solvent, catalyst and type of precursors used are the important process parameters in sol-gel technique. Moreover, drying time and temperature significantly affect the crystal growth and particle size of the composites [6]. An investigation revealed that particle size increases with the calcination temperature so, thermal treatment of the composites at moderate temperatures produces large surface area and pore size radius with lowest density. On the other hand, thermal treatment at higher temperatures results in decrease in surface area and porosity due to densification process [28]. Furthermore, the optical band gap of nanoparticles is inversely related to the particle size so increase in particle size at high calcination temperatures leads to decrease in band gap [10].

X-ray diffraction analysis

X-ray diffraction patterns were recorded to identify the phase composition of prepared composites. All the peaks were confirmed by search-match program using Bruker X-ray diffractometer (D8 Advance) software and results are presented in Fig. 2. The pattern for NCS-1 shows broad peaks at $2\theta = 37.25°, 43.28°, 62.87°, 75.09°,$ and $79.18°$ which correspond to the diffraction of [111], [200], [220], [311] and [222] planes of the cubic phase of NiO with lattice constants, $a = b = c = 4 \cdot 1771 \text{Å}$ (PDF 78-0429). These results are in close agreement with the work done by previous scientists [12, 29, 30]. Note that no peaks for tenorite (CuO) structure are observed, therefore it can be suggested that cubic crystallites of nickel copper oxide ($Ni_{90}Cu_{10}O$) may be present since its corresponding peaks appear at $2\theta = 37.21°, 43.23°, 62.80°, 75.31°$ and $79.30°$ with [101], [111], [220], [311] and [222] diffraction planes (PDF 78-0645) and hence, peaks for both the phases are superimposed by each other, as a result of which broad peaks are formed. Broadening of peaks is also attributed to the elastic strain produced in the crystal structures during growth of nanocrystals [10].

For NCS-2, similar but less intense peaks for cubic crystallites of NiO can be seen. In addition, sharp peaks appear at $2\theta = 35.54°$ and $38.70°$ which represent [311] and [222] diffraction planes of monoclinic tenorite (CuO) structure (lattice constants, $a = 4.68830 \text{Å}, b = 3.42290 \text{Å}, c = 5.13190 \text{Å}$) (PDF 48-1548). Similarly, NCS-3 is also found to have multiple phases; diffraction peaks belonging to the tenorite structure become sharper

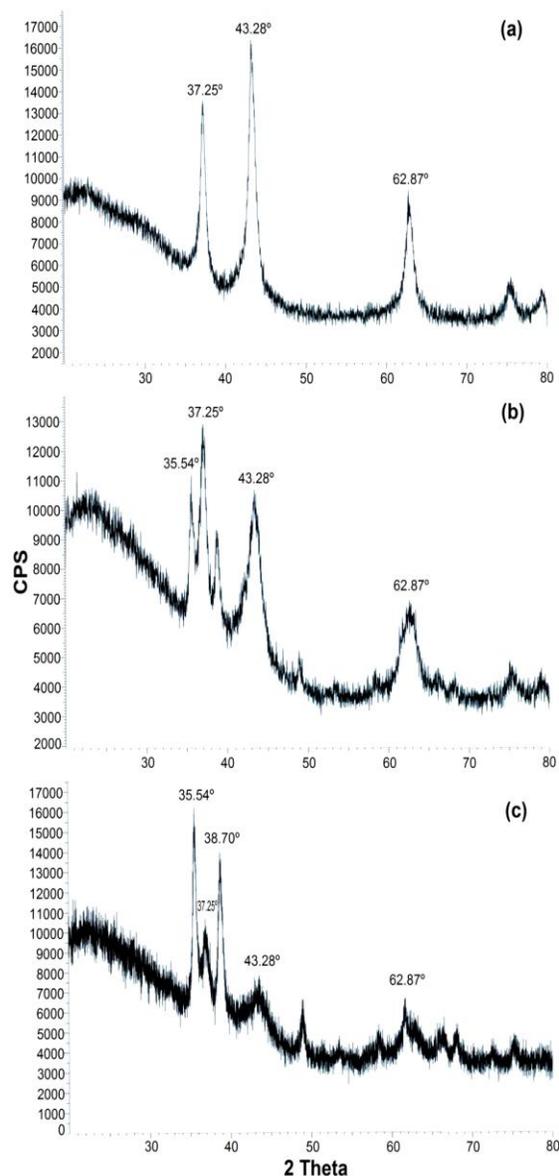whereas same peaks for nickel oxide with less intensity appear as in case of NCS-2.

Fig. 2: XRD patterns of composites (a) NCS-1, (b) NCS-2, (c) NCS-3.

It is obvious from these results that Ni_2O_3 and Cu_2O phases are not detected in any composition since, thermal treatment of the samples was carried out in air and also, no interaction of NiO and CuO precursors with the silica matrix is observed. Moreover, no peaks for crystalline SiO_2 are seen which shows that silica is in amorphous form, the reason being that silica does not crystallize at low calcination temperatures [27]; it starts crystallizing at 1000°C and completely transforms to crystalline phase cristobalite at 1100°C [31]. Other possible

reason for the absence of SiO_2 peaks may be the detection limit of X-ray diffraction technique for the crystal planes of very fine particles [27]. So, it can be inferred that all the three samples are composed of multiphase crystalline structures and broad peaks observed validate the formation of ultrafine crystallites i.e. of nanometer size.
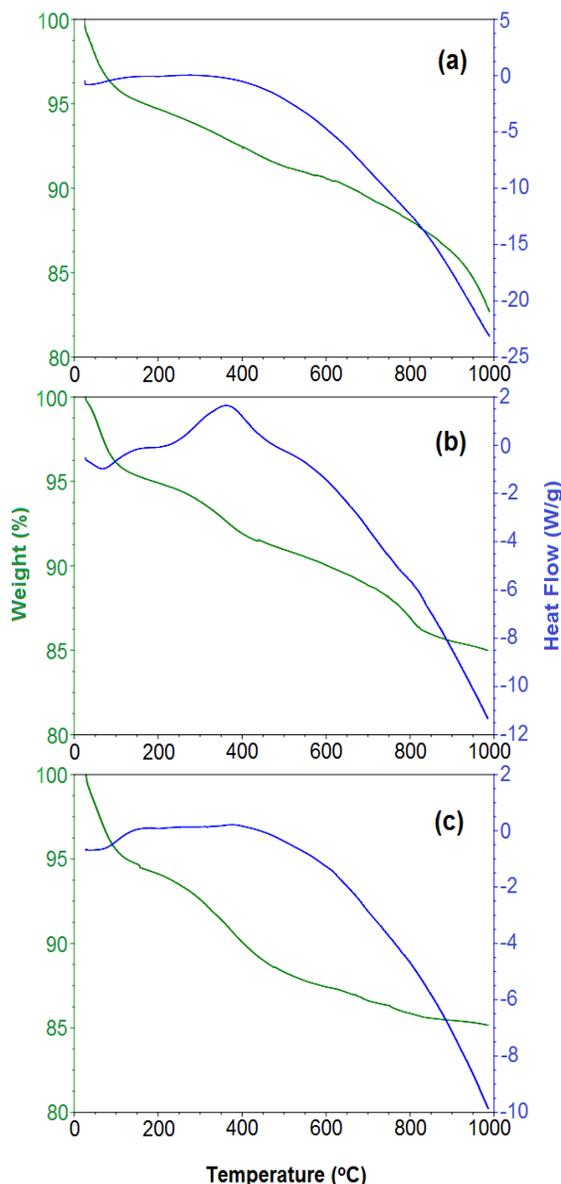

Fig. 3:   DSC-TGA curves of composites (a) NCS-1, (b) NCS-2, (c) NCS-3.

Thermal analysis

Fig.3 illustrates the heat flow and weight changes in NCS samples calcined at ambient temperature. In the first step, at lower temperature i.e. from room temperature to 100°C, a weight loss of 4-5% with a slight variation in the heat flow resulting in small endothermic peaks is observed in case of all the NCS samples due to removal of physically adsorbed water. In the temperature range of 100-400°C, a gradual weight loss of 3-6% can be seen due to the decomposition of surface hydroxyl groups and hydrogen bonded water molecules [6, 28].

In case of NCS-2 this weight loss is accompanied by a broad exothermic peak of low intensity; no prominent endothermic or exothermic peaks appear for NCS-1 and NCS-3 since the heat evolved or absorbed by the samples in DSC analyses is diffused into the material as a result of which smaller heat changes are observed [32]. At temperature ranging from 400-800°C, slow loss of 4-5% in weight of all the three samples and a further weight loss of about 4% in case of NCS-1 can be noticed probably due to the structural changes of metal oxides and dehydroxylation of silanol group (Si-OH) [6] until stable structures are formed. Topnani and co-workers also observed intense peaks between 900°C to 1000°C in DSC analyses of both CuO and Cu_2O, hence confirming the presence of monoclinic phase with self-composed structure subject to the oxidation state of copper ion [5].

Infrared spectroscopy

IR spectra of as prepared composites in the frequency range of 4000-400cm^{-1} are illustrated in Fig. 4. The spectrum for NCS-1 reveals that strong absorption bands appear below 1000cm^{-1}, in the range of 1000-1200cm^{-1}, between 2200cm^{-1} and 2400cm^{-1} and in the region above 3800cm^{-1}. NCS-2 and NCS-3 on the other hand, show different behavior as obvious from the spectra that only one distinct band between 2200cm^{-1} and 2400cm^{-1} appears while all other absorption bands diminish in both the samples. All the bands below 1000cm^{-1} can be ascribed to the bending vibrations of Cu-O and Ni-O bonds, as a previous study reveals that absorption bands associated with the vibrations of metal oxides are usually observed at frequencies less than 1000cm^{-1} [5].

The most dominant band in the range of 1000-1200cm^{-1} in NCS-1 that appears as small but broad band with slight variation in case of both NCS-2 and NCS-3 corresponds to the antisymmetric stretching vibrations of Si-O-Si bonds since the region from 400 to 1300cm^{-1} is related to the combination of vibrations of silica network [6-33]. Hossein and co-workers reported that nanocrystals of metal oxide interact with the vitreous matrix through hydroxyl groups that suggests the presence of OH

group [28]; so, it can be said that the broad absorption bands ranging from 1000-1200cm^{-1} resulted due to the overlapping of Si-O and Si-OH bands.
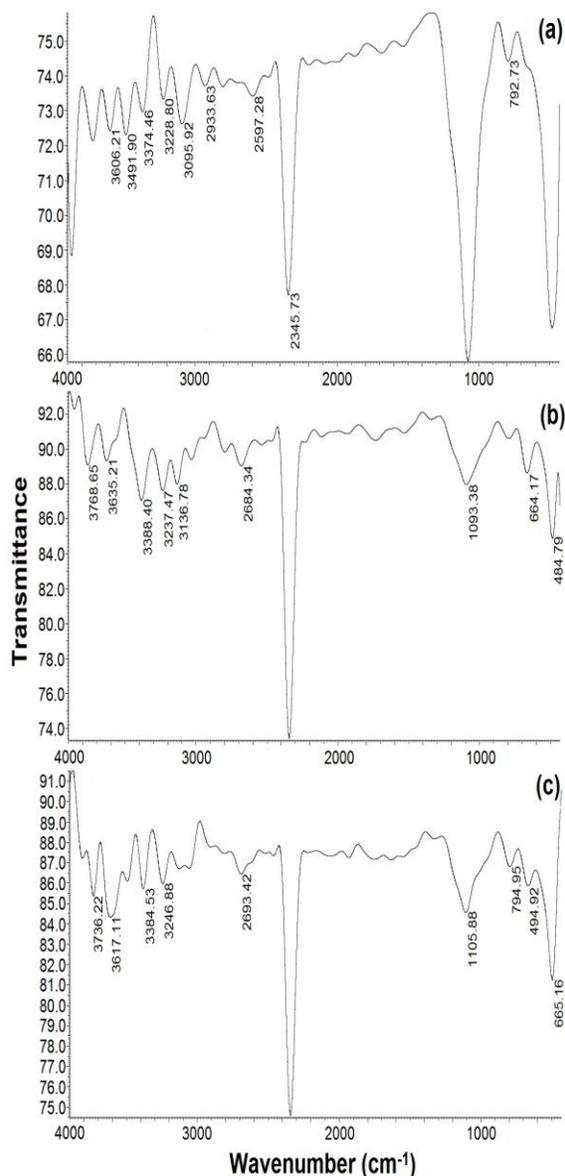

Fig. 4: IR spectra of composites (a) NCS-1, (b) NCS-2, (c) NCS-3.

The other distinct band observed between 2200-2400cm^{-1} in case of all the three NCS samples can be assigned to the overtones and combination of various vibrational modes of molecular water and SiO$_2$ network since, the frequency range from 1350cm^{-1} to 4000cm^{-1} is generally associated with these vibrations. Moreover, the high intensity of this band can be attributed to very strong hydrogen bonding resulting from the presence of free water

molecules adsorbed on the surface of the composites. The sharp absorption band above 3800cm^{-1} that can be seen in case of NCS-1 only and several small bands with varied intensities observed in the range of 2400-3800cm^{-1} can also be assigned to the overtones and combination of vibrations of Si-OH and molecular water [33].

Scanning electron microscopy

In order to confirm the composite formation, NCS-1 was subjected to scanning electron microscopy that reveals the formation of spherical shape ultrafine particles and porous structure (Fig. 5). The micrograph illustrates the amorphous morphology of silica matrix along with the silica particles agglomerated to form clusters. This cluster formation can be attributed to the large surface energy possessed by the particles during their growth that leads the particles to aggregate so as to lower their surface energy [9].

Fig. 5: SEM micrograph of composite NCS-1.

Moreover, it can be seen from the micrograph that surface of the composite is composed of metal oxide nanoparticles aggregated to form spheres of different sizes, randomly dispersed on the surface of silica matrix. The diameter of these spheres appears to be less than 100nm. The formation of relatively larger spheres is due to the fact that NiO nanoparticles are antiferromagnetic in nature [28] and thus have tendency to aggregate [34]. However, increase in diameter leads to the advantage that magnetic moment of NiO nanoparticles increases [27]. Previous researchers also had the similar observation for silica supported nickel catalysts that increase in nickel concentration leads to aggregation of nickel crystallites [35]. He and co-workers in the same way found aggregation of nickel nanoparticles over 3NiSN catalyst [36]. Likewise, copper oxide

nanoparticles tend to agglomerate easily owing to their high surface energy and large surface area resulting in the formation of larger crystallites [37]. Topnani *et al* also observed agglomerates of copper oxide nanoparticles, ranging from submicron to few microns in size. According to them this process takes place due to Ostwald ripening process [5].

Conclusions

Different compositions of NiO-CuO/SiO$_2$ composites were prepared using sol-gel technique which is the most economic and feasible method to tailor nano-size particles at low temperatures. The prepared samples were calcined at a moderate temperature i.e. 500ºC. X-ray diffraction technique confirmed the presence of amorphous silica and crystalline phases of NiO and CuO with no interaction of NiO and CuO precursors with the silica network. It can be inferred from thermal analysis that the structural changes continue to take place till the temperature is raised upto 800ºC. FTIR study revealed that water molecules were adsorbed on the surface of the prepared samples and a few of them were hydrogen bonded with each other. SEM investigation of NCS-1 proved the porous structure of sample along with the formation of metal oxide nanoparticles of spherical shape and different sizes embedded in the silica matrix because of the tendency of metal oxide nanoparticles to agglomerate easily. Since, both NiO and CuO nanoparticles are optically active so the developed composites can find application in humidity and gas sensors as well as catalysis.

References

1.   A. Kamyabi-Gol, S. M. Zebarjad and S. A. Sajjadi, A study on the effect of synthesis parameters on the size of nickel particles in sol–gel derived Ni–SiO$_2$–Al$_2$O$_3$ nanocomposites, *J. Sol-Gel Sci. Techn.*, **51**, 92 (2009).

2.   S. Nandy, S. Mallick, P. K. Ghosh, G. C. Das, S. Mukherjee, M. K. Mitra and K. K. Chattopadhyay, Impedance spectroscopic studies of nickel nanocluster in silica matrix synthesized by sol–gel method, *J. Alloy. Compo.*, **453**, 1 (2008).

3.   M. F. Casula, A. Corrias and G. Paschina, Iron oxide-silica aerogel and xerogel nanocomposite materials, *J. Non-Cryst. Solids*, **293**, 25 (2001).

4.   C. A. Canbay and A. Aydogdu, Microstructure, electrical and optical characterization of ZnO-NiO-SiO$_2$ nanocomposite synthesized by sol-gel technique. *Turk. J. Sci. Technol.*, **4**, 121 (2009).

5.   N. Topnani, S. Kushwaha and T. Athar, Wet synthesis of copper oxide nanopowder, *Int. J. Green Nanotechnol.: Mater. Sci. Eng.*, **1**, M67 (2010).

6.   M. F. Zawrah, A. A. El-Kheshen, and H. M. Abd-el-aal, Facile and economic synthesis of silica nanoparticles, *J. Ovonic Res.*, **5**, 129 (2009).

7.   T. F. Saeid and R. Ali, Green synthesis and characterization of copper oxide nanoparticles using coffee powder extract, *J. Nanostruct.*, **6**, 167 (2016).

8.   A. S. Danial, M. M. Saleh, S. A. Salih and M. I. Awad, On the synthesis of nickel-oxide nanoparticles by sol-gel technique and its electrocatalytic oxidation of glucose, *J. Power Sources*, **293**, 101 (2015).

9.   N. Srivastava and P. C. Srivastava, Realizing NiO nanocrystals from a simple chemical method, *B. Mater. Sci.*, **33**, 653 (2010).

10.   C. R. Indulal, G. S., Kumar, A. V. Vaidyan and R. Raveendran, Oxide nanostructures: characterizations and optical bandgap evaluations of cobalt-manganese and nickel-manganese at different temperatures. *J. Nano-Electron Phys.*, **3**, 170 (2011).

11.   A. Corrias, G. Mountjoy, G. Piccaluga and S. Solinas, An X-ray absorption spectroscopy study of the Ni K edge in NiO-SiO$_2$ nanocomposite materials prepared by the sol-gel method, *J. Phys. Chem. B*, **103**, 10081 (1999).

12.   H. Li, S. Zhu, H. Xi and R. Wang, Nickel oxide nanocrystallites within the wall of ordered mesoporous carbon CMK-3: synthesis and characterization, *Micropor. Mesopor. Mat.*, **89**, 196 (2006).

13.   W. Guo, K. N. Hui and K. S. Hui, High conductivity nickel oxide thin films by a facile sol-gel method. *Mater. Lett.*, **92**, 291 (2013).

14.   J. Herna´ndez-Torres and A. Mendoza-Galva´n, Formation of NiO–SiO$_2$ nanocomposite thin films by the sol–gel method, *J. Non-cryst. Solids*, **351**, 2029 (2005).

15.   B. M. Reddy, G. K. Reddy, K. N. Rao, A. Khan and I. Ganesh, Silica supported transition metal-based bimetallic catalysts for vapour phase selective hydrogenation of furfuraldehyde, *J. Mol. Catal. A-Chem.*, **265**, 276 (2007).

16.   D. Srinivas, C. V. V. Satyanarayana, H. S. Potdar and P. Ratnasamy, Structural studies on

NiO-CeO$_2$-ZrO$_2$ catalysts for steam reforming of ethanol, *Appl. Catal. A-Gen.*, **246**, 323 (2003).

17. S. Masoudian, H. H. Monfared and A. Aghaei, Silica aerogel–iron oxide nanocomposites: recoverable catalysts for the oxidation of alcohols with hydrogen peroxide, *Transit. Metal Chem.*, **36**, 521 (2011).

18. J. Jeong, J. Park, S. Choi, K. Lee and C. Lee, Catalytic effects and characteristics of Ni-based catalysts supported on TiO$_2$-SiO$_2$ xerogel, *B. Korean Chem. Soc.*, **28**, 2288 (2007).

19. R. Abbas, A. Mousa, A. Yahaya, K. Nasser, M. Mahdiyah and K. Farshid, CuO-NiO nano composites: Synthesis, characterization, and cytotoxicity evaluation, *Nanomed. Res. J.*, **2**, 78 (2017).

20. C. D. Fernández, G. Mattei, C. Sada, C. Battaglin and P. Mazzoldi, Nanostructural and optical properties of cobalt and nickel–oxide/silica nanocomposites, *Mat. Sci. Eng. C-Bio S.*, **26**, 987 (2006).

21. V. Musat, E. Fortunato, A. M. Botelho do Rego and R. Monteiro, Sol–gel cobalt oxide-silica nanocomposite thin films for gas sensing applications, *Thin Solid Films*, **516**, 1499 (2008).

22. M. Rumyantseva, V. Kovalenko, A. Gaskov, E. Makshina, V. Yuschenko, I. Ivanova, A. Ponzoni, G. Faglia and E. Comini, Nanocomposites SnO$_2$/Fe$_2$O$_3$: sensor and catalytic properties, *Sensor Actuat. B-Chem.*, **118**, 208 (2006).

23. L. Zbroniec, A. Martucci, T. Sasaki and N. Koshizaki, Optical CO gas sensing using nanostructured NiO and NiO/SiO$_2$ nanocomposites fabricated by PLD and sol gel methods, *Appl. Phys. A-Mater.*, **79**, 1303 (2004).

24. D. Buso, M. Guglielmi, A. Martucci, G. Mattei, P. Mazzoldi, C. Sada and M. L. Post, Au and NiO nanocrystals doped into porous sol-gel silica films and the effect on optical CO detection, *Nanotechnology*, **17**, 2429 (2006).

25. M. Ando, R. Chabikovsky and M. Haruta, Optical hydrogen sensitivity of nobel metal-tungsten oxide composite films prepared by sputtering deposition, *Sens. Actuators B Chem.*, **76**, 13 (2001).

26. A. Martucci, M. Pasquale and M. Guglielmi, Nanostructured silicon oxide–nickel oxide sol–gel films with enhanced optical carbon monoxide gas sensitivity, *J. Am. Ceram. Soc.*, **86**, 1638 (2003).

27. S. Chakrabarty and K. Chatterjee, Synthesis and optical manifestation of NiO-silica nanocomposite, *ISRN Nanotechnology*, **2011**, 1 (2011).

28. S. T. Hossein, G. Garnik, S. Verzhine and Z. Farhood, Effect of concentration and thermal treatment on the properties of sol-gel derived CuO/SiO$_2$ nanostructure, *Iran. J. Chem. Chem. Eng.*, **29**, 27 (2010).

29. N. M. Carneiro, W. C. Nunes, R. P. Borges, M. Godinho, L. E. Fernandez-Outon, W. A. A. Macedo and I. O. Mazali, NiO nanoparticles dispersed in mesoporous silica glass. *J. Phys. Chem. C*, **114**, 18773 (2010).

30. H. T. Rahal, R. Awad, A. M. Abdel-Gaber and D. El-Said Bakeer, Synthesis, characterization, and magnetic properties of pure and EDTA-capped NiO nanosized particles, *Journal of Nanomaterials*, **2017**, 1 (2017).

31. J. Plocek, A. Hutlova, D. Niznansky, J. Bursik, J. L. Rehspringer and Z. Micka, Preparation of CuFe$_2$O$_4$/SiO$_2$ nanocomposite by the sol-gel method, *Mater. Sci.-Poland*, **23**, 697 (2005).

32. R. C. Korošec and P. Bukovec, Sol-gel prepared NiO thin films for electrochromic applications, *Acta Chim. Slov.*, **53**, 136 (2006).

33. R. F. S. Lenza and W. L. Vasconcelos, Preparation of silica by sol-gel method using formamide, *Mater. Res-Ibero-Am. J.*, **4**, 189 (2001).

34. D. Predoi, R. Clerac, A. Jitianu, M. Zaharescu, M. Crisan and M. Raileanu, Study of Fe$_x$O$_y$-SiO$_2$ nanoparticles obtained by sol-gel synthesis, *Dig. J. Nanomater. Biostruct.*, **1**, 93 (2006).

35. B. Janković, Z. Čupić, D. Jovanović and M. Stanković, Kinetic analysis of nonisothermal reduction of silica-supported nickel catalyst precursors in a hydrogen atmosphere, *Chem. Eng. Commun.*, **203**, 182 (2016).

36. S. He, L. Zhang, S. He, L. Mo, X. Zheng, H. Wang and Y. Luo, Ni/SiO$_2$ catalyst prepared with nickel nitrate precursor for combination of CO$_2$ reforming and partial oxidation of methane: characterization and deactivation mechanism investigation, *J. Nanomater.*, **2015**, 1 (2015).

37. I. M. El-Nahhal, J. K. Salem, S. Kuhn, T. Hammad, R. Hempelmann and S. Al Bhais, Synthesis and characterization of silica-, meso-silica- and their functionalized silica-coated copper oxide nanomaterials, *J. Sol-Gel Sci. Technol.*, **79**, 573 (2016).